

# **Dynamics of Interacting Point Charges and**

## **Vortices within a constant Magnetic Field**

**Stephen Marin**

**REU Program, Summer 2005**

### **Introduction**

The problems researched and examined in this paper are useful steps to understanding why nuclear fusion is not yet a viable energy source. Fusion energy is released when, for example, two protons combine to form helium. This isotope of helium is very unstable and one proton will undergo beta decay and transform into a neutron; hence an atom composed of one proton and one neutron has been created. Two of these atoms will combine to form helium again, this time in a stable form. Fusion chains continue from this point and can cause larger and larger atoms to be formed.

As in fission, the process continues along a chain creating more stable atoms as it proceeds. Fission can be thought of as going down the chain towards lighter elements whereas fusion is climbing up the chain. The explanation is that there is an optimal atom size that maximizes stability with the strong nuclear force and the electric coulombic force. In each direction, fusion and fission, the energy released is in the form of binding energy, the energy which was previously used to keep the less stable atom together is now free. This energy takes the form of heat and once the heat is generated the fusion plant would act nearly the same as a coal or other type of power plant.

The problem is that fusion takes place in extremely hot plasma. Since the plasma is so hot, the particles it is composed of are moving fast and the fast moving particles are

difficult to trap. Through a short amount of time, atoms impact the containment vessel of the fusion reactor and the temperature of the plasma decreases leading to the cessation of fusion. A main step towards the realization of fusion power is the trapping of the plasma within the containment vessel. If it were possible to trap the plasma, binding energy could continuously be released as fusion progressed. The different problems studied in this paper logically lead to analytic and numeric study of different trapping mechanisms (which are mainly magnetic) and instabilities that occur and prevent the continuation of fusion.

### **Theory**

A few methods used in the analysis will be discussed here to allow readers to gain a greater understanding of the results. The ideas discussed in this section include linear stability analysis, real and imaginary eigen-values and their interpretation with regards to stable systems, and overview of numerical methods used in solving differential equations and comparing their accuracy.

#### **Linear Stability Analysis**

One group of systems that will be analyzed here, the charged particle systems, has a general form of a second order non-linear differential equation, which can be generalized as  $\ddot{x} = F(x)$ . This equation is simply Newton's equation of motion,  $F = ma$ , with the mass normalized to 1. To analytically solve this type of problem it is useful to apply linear stability analysis, which is described by the following.

Let  $\ddot{x} = F(x)$  where  $x = x(t)$  and  $F$  is a nonlinear function. Rewrite the differential equation as a system of first order nonlinear differential equations such that:

$$\dot{x} = v \tag{1}$$

$$\dot{v} = F(x) \quad (2)$$

To make this a linear system, the function  $F$  must now be Taylor expanded around the equilibrium point to be analyzed (for this paper there will be only one equilibrium point in each system). As an approximation, keep only up to the linear term of the expansion.

Now the system can be written as:

$$\dot{\bar{x}} = A\bar{x} \quad (3)$$

where  $A$  is a linear matrix known as the stability matrix. Finally find the eigen-values of  $A$  by solving for the roots of the characteristic polynomial  $\det(A - \lambda I) = 0$  for  $\lambda$ . The linear stability can now be determined by analyzing the eigen-values.

### Real and Imaginary Eigen-Values

In a linear system of differential equations, eigen-values dictate the way in which the solution acts. In a linear system, general solutions are of the form

$$x(t) = c_1 e^{\lambda_1 t} + c_2 e^{\lambda_2 t} + c_3 e^{\lambda_3 t} + \dots + c_n e^{\lambda_n t} \quad (4)$$

where  $n$  is the order of the system and the  $\lambda$  are the eigen-values found in the previous section.

How the solution responds, whether it is stable or not, depends upon the eigen-values and the initial conditions. If the eigen-values are purely real and positive then the system is unbounded. If eigen-values are purely real and negative the system will be bounded by its initial conditions and will tend towards a single point. Finally, if they are purely imaginary the system will oscillate around some point (this is due to Euler's equation  $e^{it} = \cos(t) + i \sin(t)$ ).

If the eigen-values are a mixture of the 3 types noted above then the initial conditions must be used to find the general behavior of the system. Once the general solution is found, the initial conditions are used to evaluate the constants  $c_1, c_2, \dots, c_n$ . For example, in a second order system there may be one positive and one negative eigen-value. Therefore it would seem the system would be unbounded, but the initial conditions could lead to the constant before the positive eigen-value evaluating to zero. Thus the system would converge to a point.

### Overview of Numerical Methods

Numerical methods are tools that are used when a system of differential equations is either difficult or improbable to solve. Three common methods are Euler's method, the Improved Euler Method, and the Runge-Kutta (RK4) method. Generally these methods all use the same technique to evaluate a function from a differential equation. First they all evaluate the slope, or  $\dot{x}$ , at some initial time  $t_n$ . Then using the step size  $h$  the slopes at future times are approximated. For Euler's Method the step size is multiplied by the slope to approximate the function over the step size interval. For the Improved Euler's Method, the slope is averaged between time  $t_n$  and  $t_{n+1}$  using a step of Euler's Method to approximate the slope at  $t_{n+1}$ . Finally, for the Runge-Kutta Method (RK4) the slope is approximated four times and a weighted average of the slopes is taken. How each method goes from some time  $t_n$  to the next time  $t_{n+1}$  can be seen below.

**Euler's Method:** 
$$x_{n+1} = x_n + hf(t_n, x_n) \quad (5)$$

**Improved Euler's Method:**

$$x_{n+1} = x_n + \frac{h}{2}[f(t_n, x_n) + f(t_{n+1}, x_n + hf(t_n, x_n))] \quad (6)$$

$$\text{Runge-Kutta Method: } x_{n+1} = x_n + \frac{h}{6}(k_1 + 2k_2 + 2k_3 + k_4) \quad (7)$$

$$k_1 = f(t_n, x_n) \quad (7a)$$

$$k_2 = f\left(t_n + \frac{h}{2}, x_n + \frac{h}{2}k_1\right) \quad (7b)$$

$$k_3 = f\left(t_n + \frac{h}{2}, x_n + \frac{h}{2}k_2\right) \quad (7c)$$

$$k_4 = f(t_n + h, x_n + hk_3) \quad (7d)$$

where  $h$  is the time step, which is the number of steps taken to get from the initial time to the final time divided by the difference in time, or the interval in time between steps.

The order  $p$  of the approximation is a constant associated with the accuracy of the approximation. These three methods will be tested against each other for the problem  $\dot{x} = x$  with initial condition  $x(0) = 1$  (This is the function  $x(t) = e^t$ ). The final time in this approximation is  $t = 1$ , so this ultimately is just an evaluation of the number  $e$ . As can be see in figure 1 (which is a log-log plot), the Improved Euler's Method is better than Euler's Method and RK4 is much more accurate for a given time step  $h$  than both other methods.

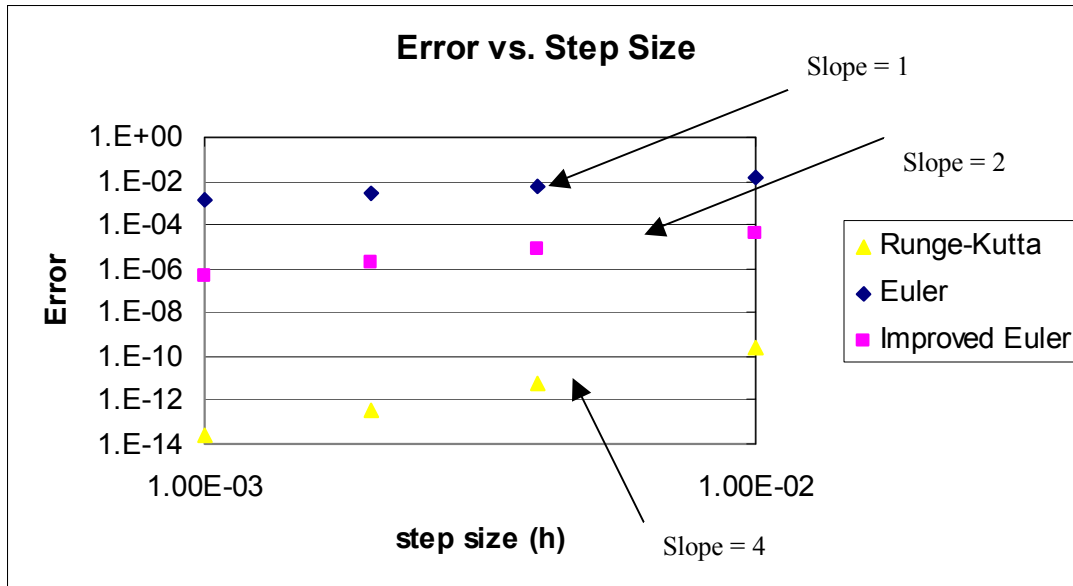


Figure 1 shows the error in approximation of the number  $e$  on a log-log scale.

Each of these numerical methods is defined by a number  $p$  called the order. The order is important because for each method the error divided by the step size to the power of the order,  $\frac{Error}{h^p}$ , is a constant (as can be seen in figure 2), where the orders of Euler's, the Improved Euler's, and RK4 methods are 1, 2, and 4 respectively. Hence when the step size for Euler's method is decreased by a factor of 10, the error should also decrease by a factor of 10. However for RK4, a decrease in step size by a factor of 10 decreases the error by a factor of 10,000. While each time step of RK4 has more calculations that must be made when compared to the other two methods, the increase in the approximation often offsets the increased calculation time.

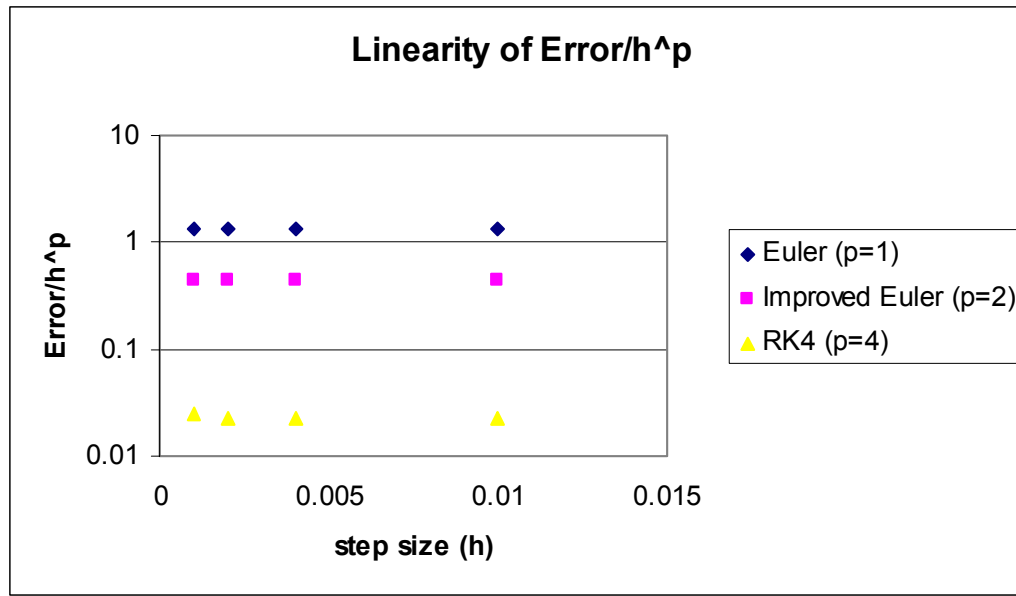


Figure 2 shows the linearity and order of 3 numerical methods used for solving differential equations

### The Electric Charge Systems

Systems composed of electric charges will be the first type examined here. We will examine four different setups of this problem; two will have two stationary particles, one will have one stationary particle, and one will have no stationary particles. Before we examine any of these systems, we must first describe the basic setup.

For all four variations on this system, the initial setup will follow figure 3. The only parameters that will change are which particles are fixed, the values of  $d_1, d_2, q_1, q_2$  and  $q_3$  which are the distances between the point charges and the charge of the particles respectively.

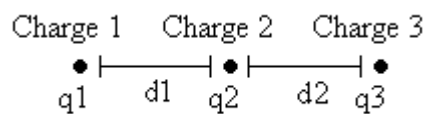


Figure 3 Initial Setup of the 3 charge system

Furthermore, all steady state solutions must be examined. Assume all three charges lay along the  $x$ -axis and placement of charges 1, 2 and 3 are  $x_1, x_2$ , and  $x_3$  respectively.

Then, the net forces on particles 1, 2, and 3 are:

$$F_1 = C |x_1 - x_2| \frac{q_1 q_2}{(x_1 - x_2)^3} + C |x_1 - x_3| \frac{q_1 q_3}{(x_1 - x_3)^3} \quad (8a)$$

$$F_2 = C |x_2 - x_1| \frac{q_2 q_1}{(x_2 - x_1)^3} + C |x_2 - x_3| \frac{q_2 q_3}{(x_2 - x_3)^3} \quad (8b)$$

$$F_3 = C |x_3 - x_1| \frac{q_3 q_1}{(x_3 - x_1)^3} + C |x_3 - x_2| \frac{q_3 q_2}{(x_3 - x_2)^3} \quad (8c)$$

where  $C$  is the constant  $\frac{1}{4\pi\epsilon_0}$  and  $\epsilon_0$  is the permittivity constant. Due to symmetry, the

distance between particles 2 and 3 must be the same as the distance between particles 1 and 2. Let this distance be denoted  $d$ . Again for the sake of symmetry, the charge on particle 1 must equal the charge on particle 3. After these simplifications are made, it is

found that the charge on particle 2 must equal one quarter of the charge of particles 1 and

3. To summarize the steady state solution requires a setup where  $d_1 = d_2 = d$ ,  $d > 0$ , and

$q_1 = q_3 = \frac{-q_2}{4}$ . All approximations from this point forward will be made using Matlab

and the RK4 numerical method

**Case 1a: Horizontal Motion,**  $q_1 = q_3 = \frac{-q_2}{4}$

The first variation that will be studied consists of one particle moving horizontally. Let the system assume the steady state configuration and let particles 1 and 3 be fixed at positions  $d$  and  $-d$  on the  $x$ -axis. From this setup, charge 2 will be displaced

along the  $x$ -axis. This displacement must be small with relation to  $d$ , because the linear stability analysis was taken around the stable point with charge 2 located at  $x_2 = 0$ . The linear stability analysis for this setup resulted in real eigen-values which are  $\lambda_{1,2} = \frac{\pm 2}{d^{3/2}}$ , therefore the solution will either tend towards 0, the stable point, or will be unbounded. With the initial conditions  $x_2(0) = x_{2_0}$  and  $\dot{x}(0) = 0$ , the general solution becomes:

$$x_2(t) = \frac{x_{2_0}}{2} (e^{\lambda_1 t} + e^{\lambda_2 t}) \quad (9)$$

Therefore the positive eigen-value will out weigh the negative eigen-value and this system will be unbounded. Figure 4 demonstrates this exponential behavior with the initial conditions stated above and with  $x_{2_0} = 1, d = 7, h = 0.001$  and  $t_{final} = 30$ .

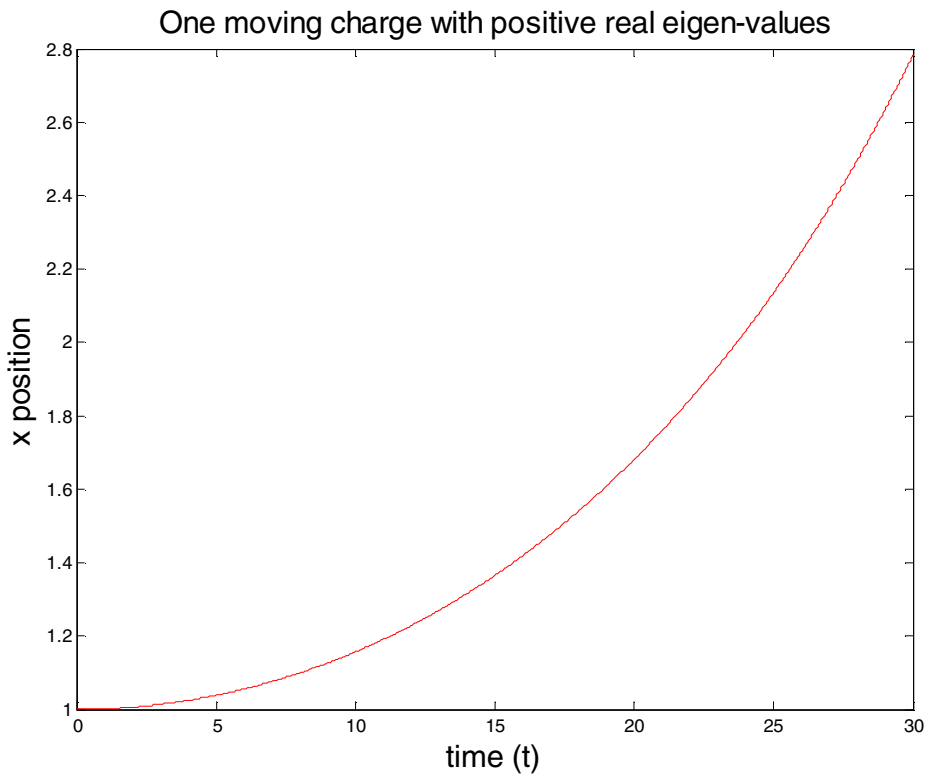


**Figure 4 depicts unbounded growth due to positive real eigen-values**

If the initial conditions are changed so that  $x_2(0) = x_{2_0}$  and  $\dot{x}(0) = -\lambda x_{2_0}$ , then the coefficient associated with the positive eigen-value will be zero. Therefore the general solution will become:

$$x_2(t) = x_{2_0} e^{\lambda_2 t} \quad (10)$$

Thus the system is bounded by  $x_2(0) = x_{2_0}$  and will tend towards 0 for all time  $t$  greater than 0. Figure 5 demonstrates this behavior.

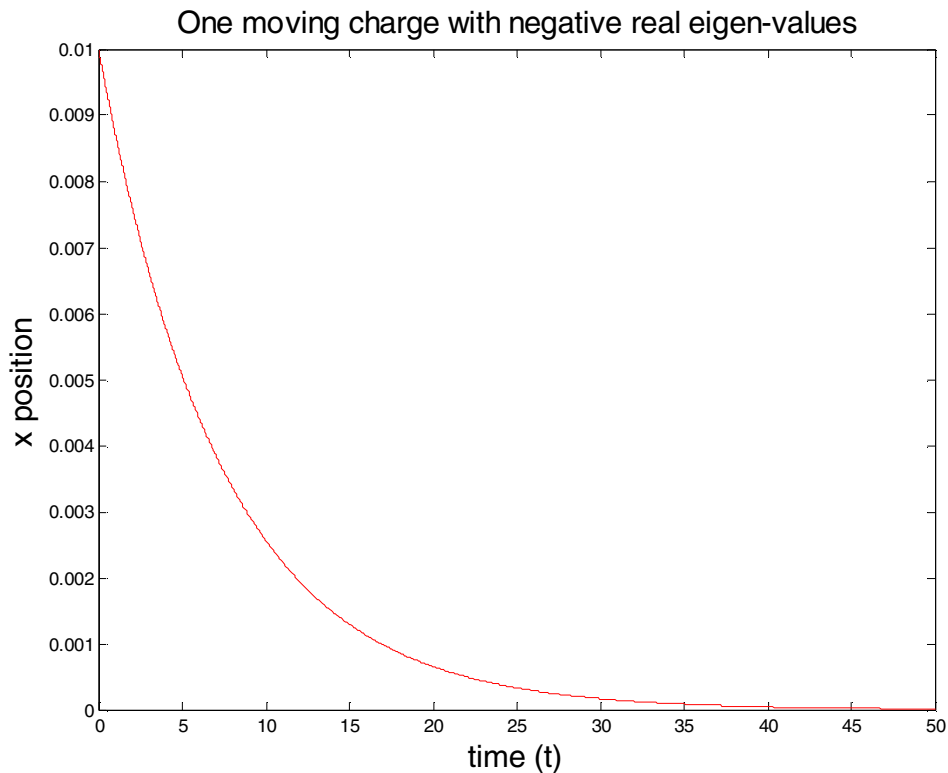


Figure 5 depicts the bounded nature of negative real eigen-values

**Case 1b: Horizontal Motion,**  $q_1 = q_3 = \frac{q_2}{4}$

The next setup examined is the same as above except the charge on particle 2 has been changed to the opposite sign,  $q_1 = q_3 = \frac{q_2}{4}$ . The linear stability analysis of the setup

is the same except when the determinant is taken,  $\lambda^2 = \frac{-4|q_1q_2|}{d^3}$ , whereas in the above

system  $\lambda^2 = \frac{4|q_1q_2|}{d^3}$ . The eigen-values for this system are  $\lambda = \frac{\pm 2i|q_1q_2|^{1/2}}{d^{3/2}}$ . By

Euler's equation, the general solution becomes:

$$x_2(t) = A \cos(\lambda t) + iB \sin(\lambda t). \quad (11)$$

With initial conditions  $x_2(0) = x_{2_0}$  and  $\dot{x}(0) = 0$ , equation (11) becomes:

$$x_2(t) = x_{2_0} \cos(\lambda t) \quad (12)$$

where  $\lambda$  is related to the frequency  $\omega$  by  $\lambda = \omega^2$ . The system described by equation (12) is an oscillatory system which can be seen in figure 6.

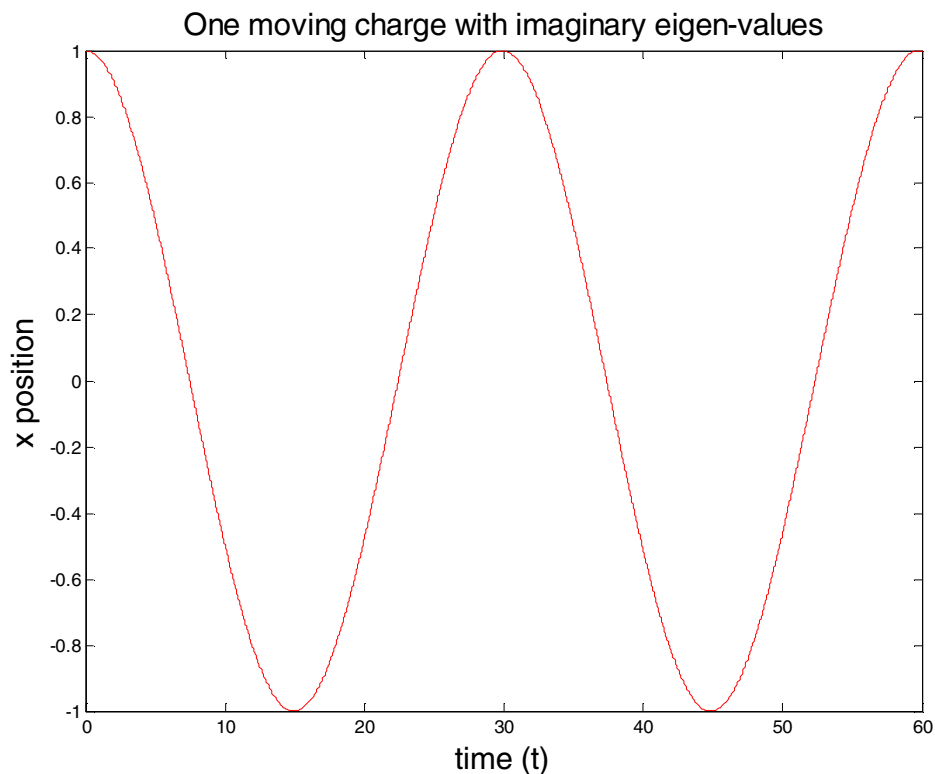


**Figure 6 depicts the oscillatory aspects of imaginary eigen-values**

**Case 2a: Vertical Motion,**  $q_1 = q_3 = \frac{-q_2}{4}$

Here we will study the same system as in case 1, except particle 2 will be moving vertically with opposite charge. Linear stability analysis results in imaginary eigenvalues, which lead to an oscillatory system which can be seen in figure 7. The general motion of this case is similar to the motion of case 1b, where particle 2 had the same sign and moved horizontally.

**Case 2b: Vertical Motion,**  $q_1 = q_3 = \frac{q_2}{4}$

Case 2b consists of the setup from figure 3, where the charge on particle 2 has the same sign as particles 1 and 3, and particle 2 is displaced vertically. Opposite from case 2a, the linear stability analysis for this case results in purely positive (and real) eigenvalues and an unstable system which can also be seen in figure 7. This case has a similar motion as case 1a.

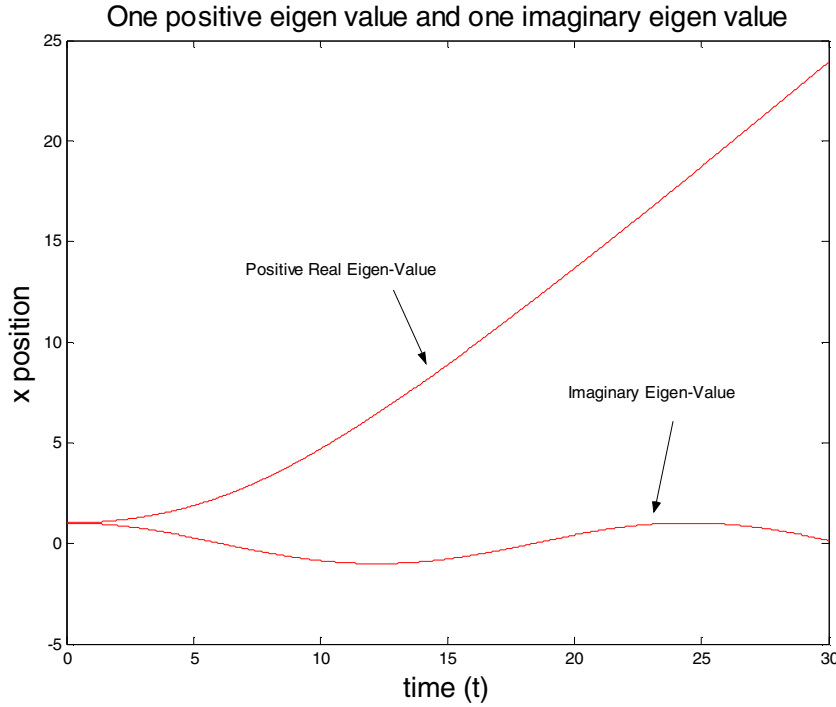


Figure 7 shows both the stable and unstable setups of the vertically moving particle

### Case 3 : Particle 2 remains fixed, and Particles 1 and 3 are free to move

Thirdly, we will examine a system which has the initial setup of figure 3, except particle 2 will now be fixed and particles 1 and 3 will be free to move horizontally. A distinction must be made here that this system is now described by two second order differential equations.

$$\ddot{x}_1 = F_1(x_1, x_3) = C |x_1 - x_3| \frac{q_1 q_3}{(x_1 - x_3)^3} + C |x_1| \frac{q_1 q_2}{(x_1)^3} \quad (13a)$$

$$\ddot{x}_3 = F_3(x_1, x_3) = C |x_3 - x_1| \frac{q_1 q_3}{(x_3 - x_1)^3} + C |x_3| \frac{q_3 q_2}{(x_3)^3} \quad (13b)$$

To complete the linear stability analysis, first order Taylor expansions must be taken around the stable point, which is  $(x_1, x_3) = (-d, d)$ . Once this linear stability analysis is completed, the eigen-values are found to be:

$$\lambda_{1,2,3,4} = \frac{\pm \sqrt{q_1} \sqrt{-8q_2 \pm |q_3| - q_3}}{2(|d|)^{3/2}} \quad (14)$$

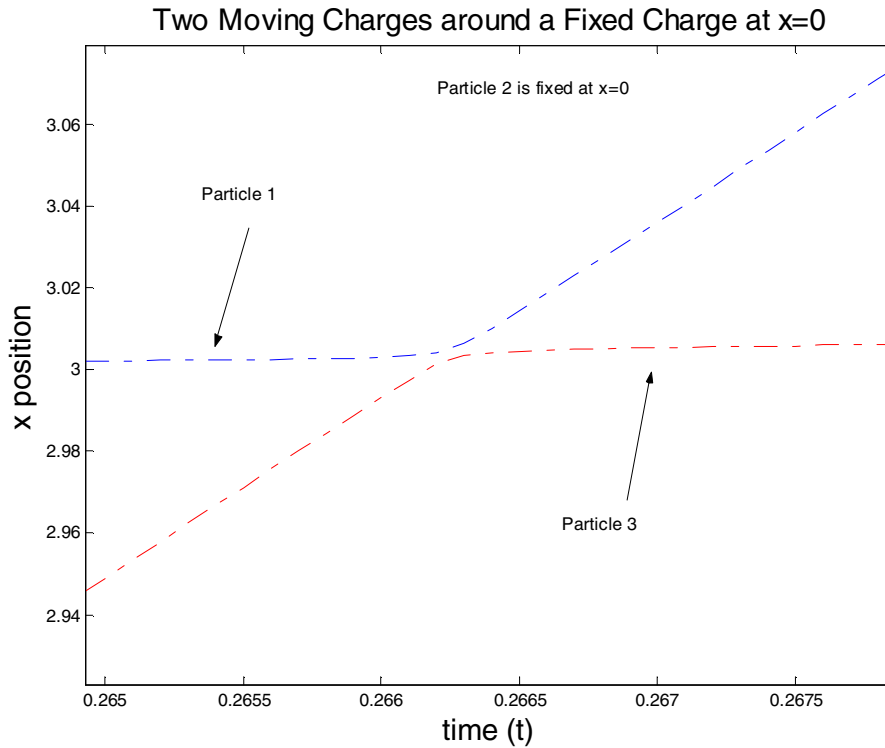


**Figure 8 shows a collision between 2 charges,  $q_1 = q_3 = -q_2/4$**

Figure 8 was generated by setting the system to the equilibrium point and then giving particle 1 (which was initially at  $x = -3$ ) a velocity of 15. The time step for this graph was  $h = 0.001$ , and this time step allowed particle 1 to step over particle 2. Without a finite time step, particle 1 could not have stepped over particle 2. One important note to recognize is that one can see from just looking at the plot that momentum is conserved. The force from particle 2 can be neglected, because the collision occurs very far from particle 2. Therefore the forces exerted on each particle are so large that the force from particle 2 is negligible.

#### Case 4: All three particles are free to move

The final system that will be examined in this section follows the initial setup of figure 3, but now all three particles are free to move. This system was not analyzed using linear stability analysis due to the amount of work required, however the results are reliable. The code for this setup was modeled after the code for all previous configurations, which were all analyzed with linear stability analysis and fit well with the expected results. Once again a finite step size allows particles to step over other particles.

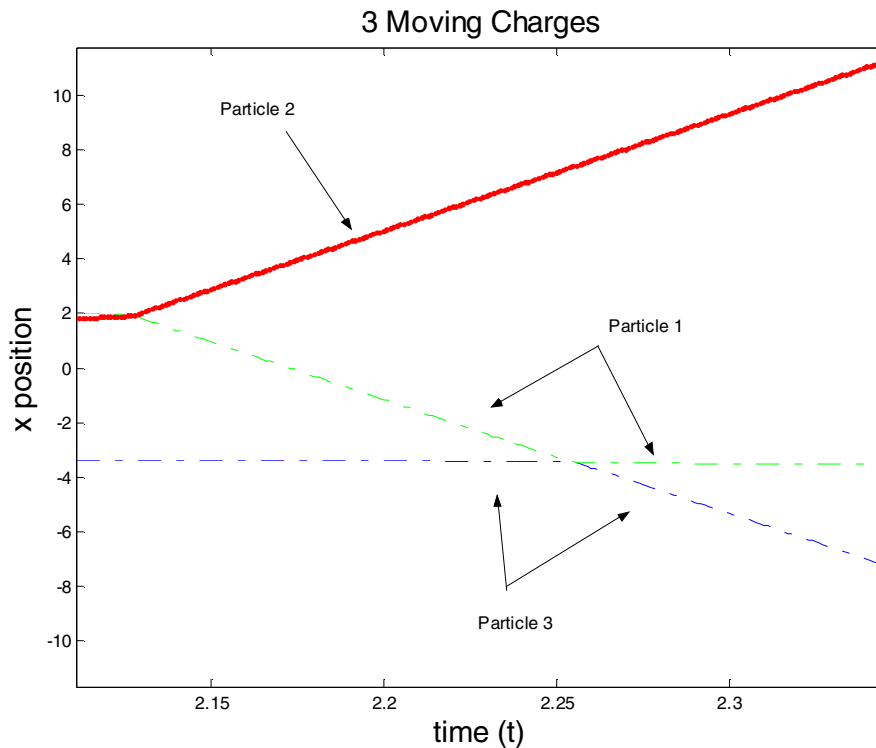


**Figure 9 shows the interaction of 3 freely moving charges in one dimension**

Figure 9 was generated from the equilibrium position with  $d = 3$  and then particle 2 was displaced to  $x = 0.5$ . The charges on the three particles were  $q_1 = q_3 = 4$ , and  $q_2 = -1$ .

The step size was  $h = 0.001$ .

To begin, charges 1 and 2 cross. Since they have opposite charge, they accelerate as they pass one another. Then the accelerated charge 2 collides with the relatively stationary charge 3. Charge 3 absorbs most of the kinetic energy from charge 1 and escapes the system along the negative  $x$  direction.

### **Vortex Systems**

In this section the analysis will center on point-like vortices within a constant magnetic field with no background plasma. A fundamental difference between this section and the previous section dealing with electric charges, is that this section will deal with induced velocity fields whereas the last section dealt with forces. Given a group of  $n$  vortices in a magnetic field, the motion of the  $i$ th vortex depends on the electric field induced by the other vortices and the magnetic field. This can be written as:

$$v_i = \frac{\vec{E}_i \times \vec{B}_z}{|\vec{B}_z|^2} \quad (15)$$

where  $E_i$  is the electric field at particle  $i$  and  $B_z$  is the magnetic field in the  $z$ -direction. Equation (15) describes the exact means by which the drift velocity can be found. The first thing to note is that (with the electric field solely in the  $x$ - $y$  plane) the magnetic field involved in the drift velocity is perpendicular to the electric field, the  $z$  vector. Furthermore the drift velocity is perpendicular to both the electric field at vortex  $i$  and the  $z$  portion of the magnetic field. As noted above, this analysis will lead to an induced velocity field, defined by the following set of equations:

$$\dot{x}_i = v_{x_i} = -E_{i_y} \quad (16a)$$

$$\dot{y}_i = v_{y_i} = E_{i_x} \quad (16b)$$

where  $E_{i_y}$  and  $E_{i_x}$  are the  $x$  and  $y$  components of the electric field at vortex  $i$ . The  $x$  portion of the electric field can be found with the summation:

$$E_{i_x} = \sum_{n=1, n \neq i}^n \frac{q_n}{\epsilon_0} \frac{x_i - x_n}{((x_i - x_n)^2 + (y_i - y_n)^2)} \quad (17)$$

with  $q_n, \epsilon_0$ , and  $x_i$  representing the magnitude of vortex  $n$ , the permittivity of free space, and the  $x$  placement of vortex  $i$  respectively. For the ease of calculation the magnetic field has been normalized to one Tesla. A similar summation is taken for the  $y$  portion of the electric field with  $y_i$  replacing  $x_i$ . For the numerical analysis this summation is repeated for all  $n$  particles.

The above analysis leads to the first conclusion of this section. With one vortex fixed at the origin and one free vortex both in the  $x$ - $y$  plane with constant magnetic field acting along the  $z$ -axis, the induced motion of the free vortex will follow a circular path.

Figure 10 shows the vortex rotating counter-clockwise. If the opposite magnitude of the vortex were taken, it would rotate clockwise. Figure 8 was generated using a final time of 10, a step size of  $h = 0.001$ , and the vortex was initially at point (1,1).

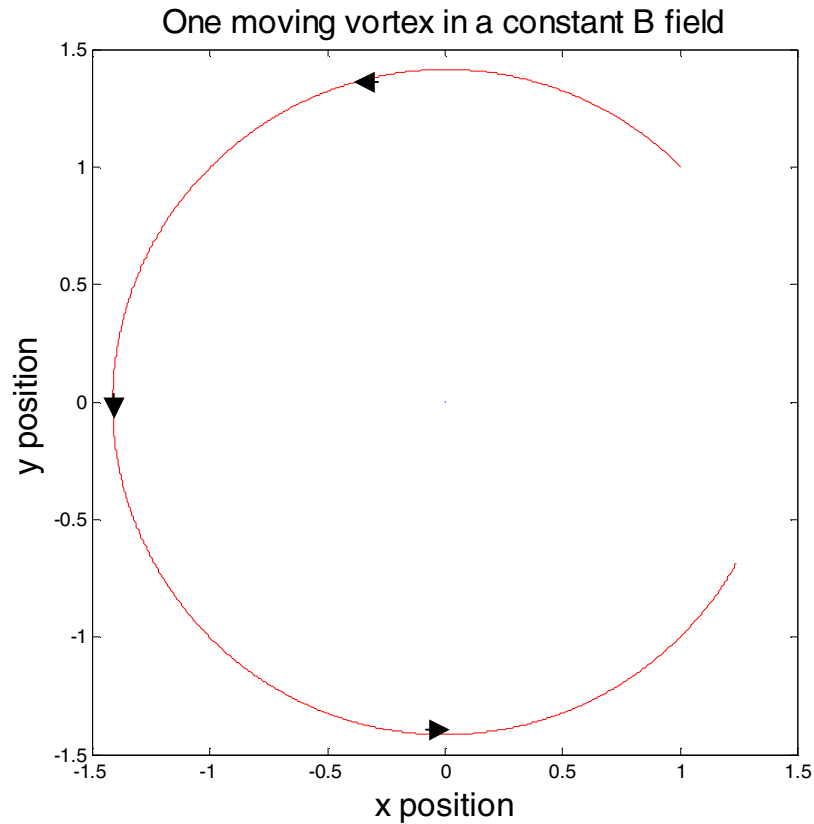


**Figure 10 shows the motion of one vortex through time with a constant magnetic field**

When two vortices are free to interact and move, two general types of behavior are seen. If the two vortices have the same magnitude then they will simply rotate about a common center as seen in figure 11. Alternatively if the two vortices have the opposite magnitude they will propagate together; this can be seen in figure 12.

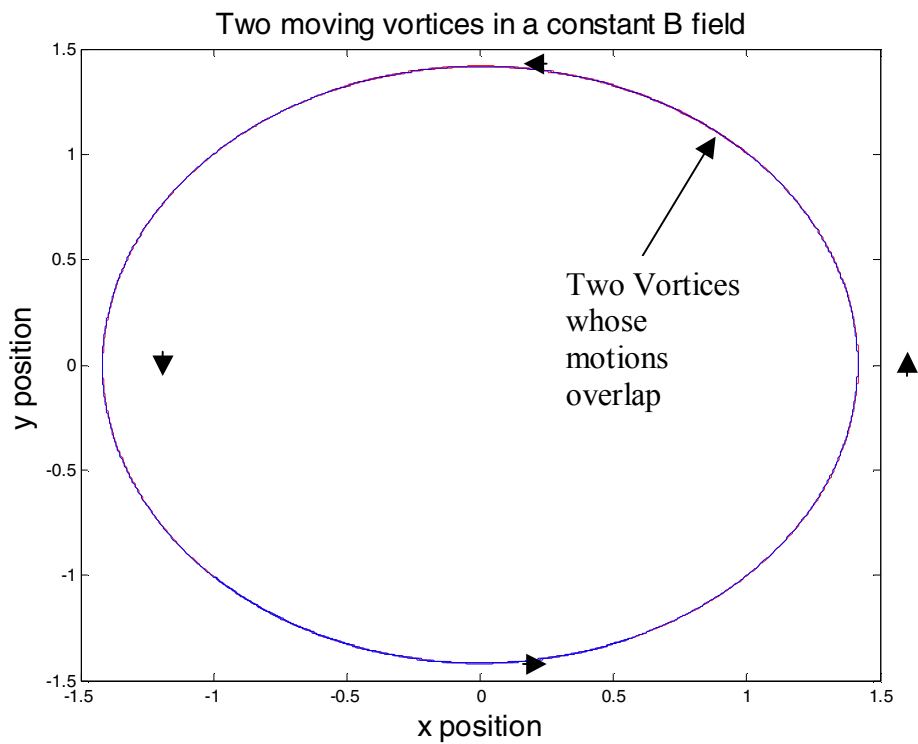


Figure 11 shows rotational behavior of two vortices with the same magnitude and same sign

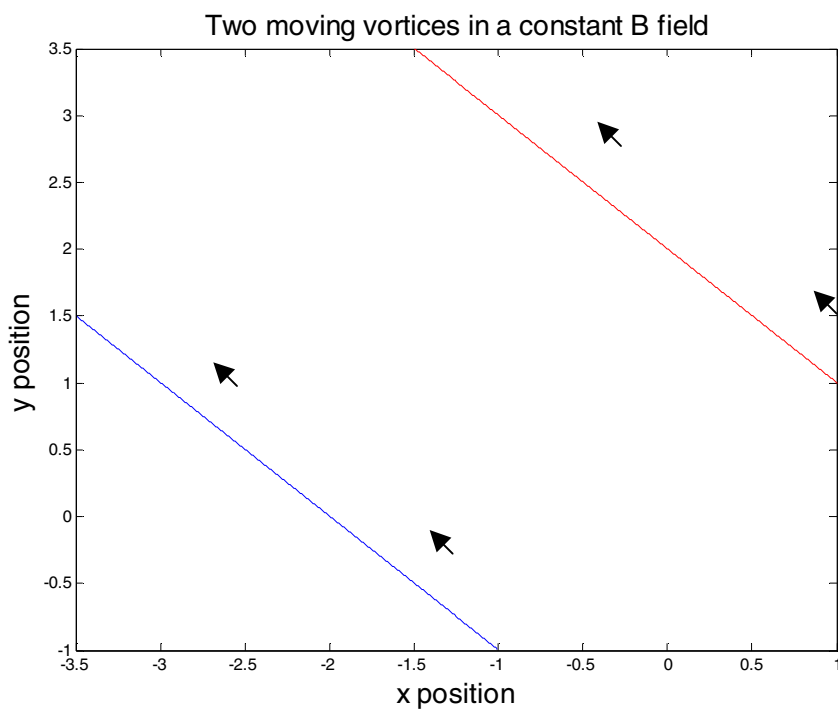


Figure 12 depicts the propagation of 2 vortices with same magnitude and opposite sign

Let the initial placement of vortex  $i$  be denoted  $V_i(0) = (x, y)$ . Then for figures 11 and 12  $V_1(0) = (1,1)$  (with magnitude 1 for figure 11 and -1 for figure 12) and  $V_2(0) = (-1,0)$  with magnitude 1. For both figures,  $t_{final} = 10$  and  $h = 0.001$ .

An interesting feature arises when the magnitudes of the two vortices are almost, but not quite, opposite one another. When this happens, both types of motion can be seen, propagation and rotation. Figure 13 shows such an occurrence with  $V_1(0) = (1,1)$ ,  $V_2(0) = (-1,0)$ ,  $t_{final} = 10$ , and  $h = 0.001$ . The magnitude of vortex 1 equals -20.5 and the magnitude of vortex 2 is 20.

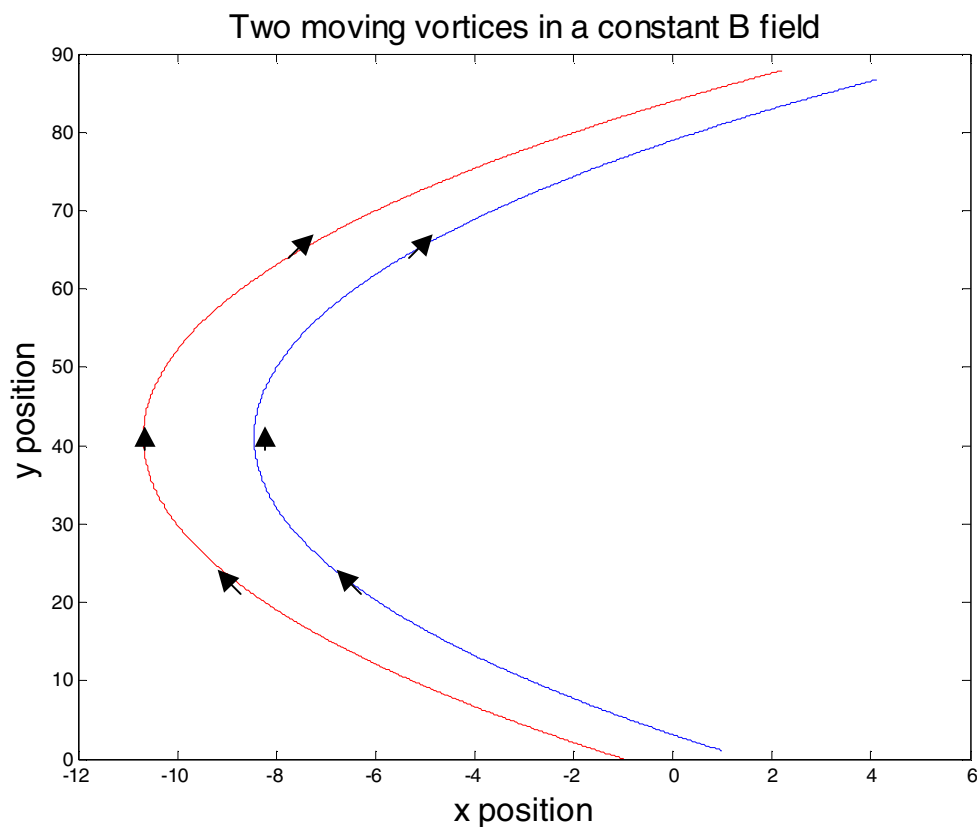
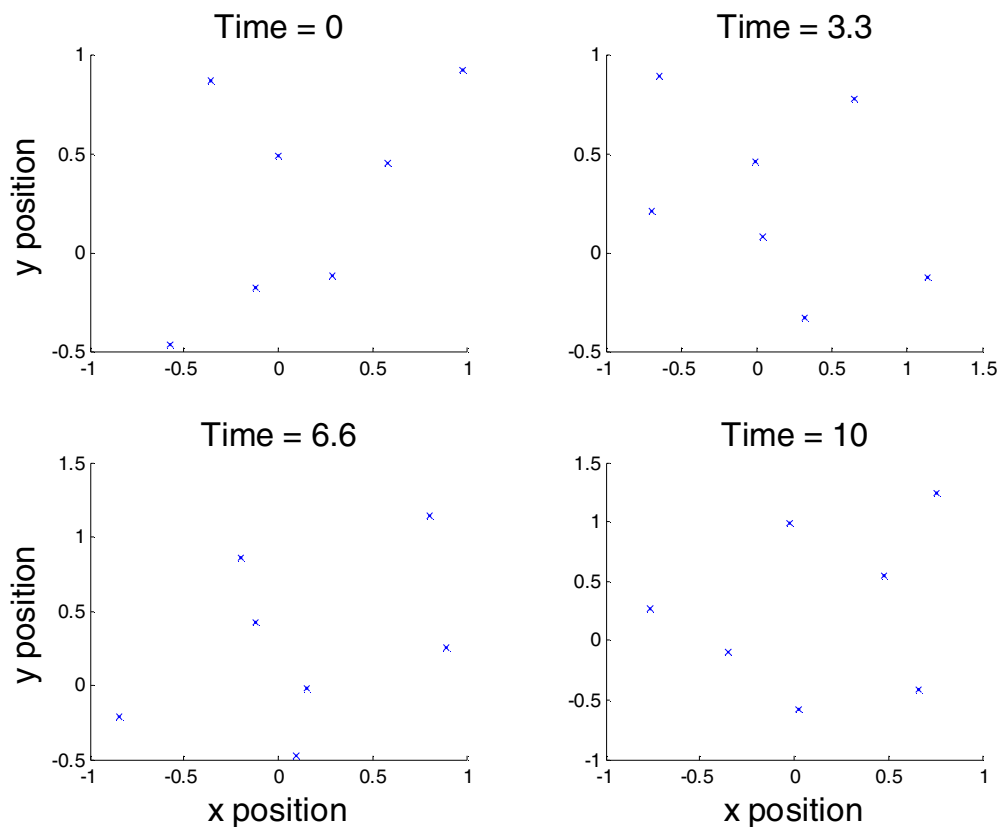


Figure 13 shows both the propagation and rotation properties

Finally, a system with seven vortices will be examined. Once again, no analysis has been done for this system beyond the numerical analysis seen below. Yet, the results seen here should be trusted. The above systems were analyzed with theory so that trust could be given to them, and the seven vortex system was built upon the tested versions. Following this method provides reason to trust a method that was not, or could not, be solved through some exact form.

When all 7 vortices have the same magnitude, a rather chaotic motion can be seen. Below, figure 14, shows a time slice of the motion of the seven vortices. Figure 14 also shows that through time the orientation of the seven particles remains random, and, without a background plasma, no crystallization occurs.



**Figure 14 is a time slice of the motion of seven vortices in a constant magnetic field**

The entire motion of the seven vortex system is shown in figure 15. As can be seen, the motion is quite chaotic. A few notes that should be made are that the system will continue to expand and will not form a crystalline structure. The system is unstable, and, lacking a background plasma, cannot become stable.

### Seven Vortices with the same Sign and Magnitude in a constant Magnetic Field

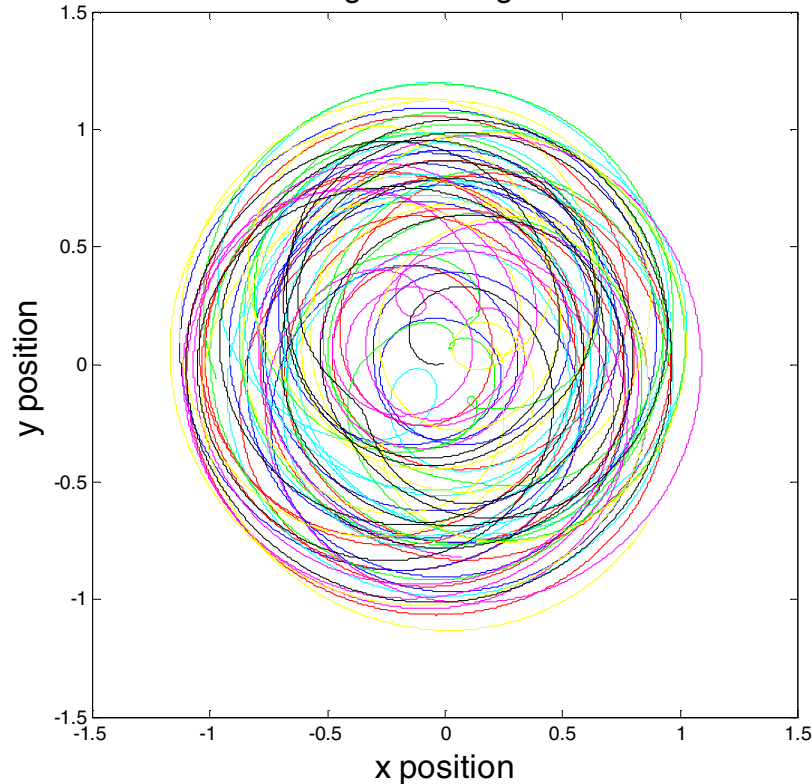


**Figure 15 is the entire motion for a time of 10 units of 7 vortices in a constant magnetic field**

However, when vortices have both positive and negative magnitudes, those with opposite magnitudes pair together to form a vortex dipole and propagate out of the system together. Once the dipoles leave the system, only one vortex remains, and, having no electric field, the remaining vortex has no velocity.

### Seven Vortices with Opposite Magnitudes in a constant Magnetic Field

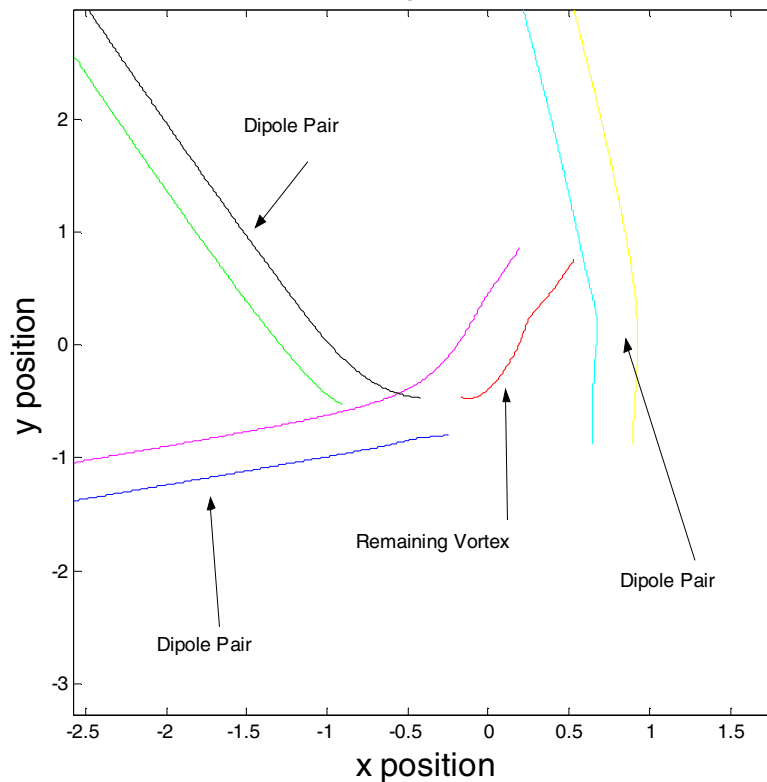


**Figure 16 shows vortex dipole pair**

The system in figure 16 is composed of seven vortices. All vortices have the same magnitude, while four vortices have a positive sign and three have a negative sign. The one remaining vortex is the fourth positive vortex that did not form a dipole. With no electric field, the remaining vortex will have no induced velocity.

### **Conclusions and Where This Leads**

The work provided here was largely an end in itself. Many of the solutions are neither deep nor sophisticated; however they provide an immense foundation for exploration into many different areas. The electric charge systems led into a study of the systems of vortices and the study of vortices leads to many interesting topics. Such topics include study of self regulating vortices within a vortex and the two stream

instability. Also, the study of numerical methods that was done leads to other interesting topics. A couple of ideas that could be examined further are how the period of an oscillatory electric charge system predicted linear stability would compare to the period from a numerical method. The period found from the numerical method could be a function of many different variables, most notably the time step.

Some concrete conclusions found in this paper involve the three charge system, the seven vortex system, and a working code of RK4 to be used on a second order system of differential equations. The steady state of the three charge system is independent of the variable  $d$ . Also there is another degree of freedom in selecting the charge of either the interior or exterior charges in figure 3. For the seven vortex system, the lack of self regulation without a background plasma is an interesting discovery. Without the background plasma, there is no means by which the vortices can expel substance from the system in an effort to align in a crystalline form. The pairing that was seen when oppositely or nearly oppositely charged vortices near each other in a magnetic field is a further discovery. Finally a working algorithm for using RK4 on a second order differential equation is an extremely useful tool.

I feel the most important things I learned while working on the material covered in this paper revolve around the practice I received with my problem solving. Coming into the REU program, I had only slight practice with Matlab and now I feel very comfortable programming and I believe that the understanding I gained through this program will allow me to solve many more difficult problems that I will encounter. Furthermore, I learned a great deal about linear stability analysis and how to linearize and

solve systems with as many as four eigen-values. And, finally, all that I have learned about plasma physics will be extremely helpful in my future.

In the future, I would like to examine trapping mechanisms used in an attempt to capture the plasma used in fusion as well as examine many of the instabilities that are encountered. Lastly, I also find the self regulation of vortices within a vortex highly interesting. The experience I have been lucky to receive will be immensely helpful in further study of these problems.

### **References**

Chen, Francis F., Introduction to Plasma Physics and Controlled Fusion, New York:

Plenum Press, 1984

Durkin, D., and J. Fajans, "Experimental Dynamics of a Vortex within a Vortex,"

Physical Review Letters, 85(19), (2000): 4052-5.

Edwards, H., and D. Penney., Differential Equations, Computing and Modeling 3<sup>rd</sup>

Edition, New Jersey: Prentice Hall, 2004.

### **Thanks**

I would like to extend my deepest heartfelt gratitude to Professors Robert Krasny and Andrew Christlieb. They have exemplified the true meaning of patience and care with me during the course of this program and I will be forever grateful for their efforts.